



HAL
open science

Historical stained-glass window laser preservation: The heat accumulation challenge

Evan Maina Maingi, María Pilar Alonso, Luis Alberto Angurel, Md Ashiqur Rahman, Rémy Chapoulie, Stéphan Dubernet, Germán Francisco de la Fuente

► To cite this version:

Evan Maina Maingi, María Pilar Alonso, Luis Alberto Angurel, Md Ashiqur Rahman, Rémy Chapoulie, et al.. Historical stained-glass window laser preservation: The heat accumulation challenge. *Boletín de la Sociedad Española de Cerámica y Vidrio*, 2022, 61 (Suppl 1), pp.S69-S82. 10.1016/j.bsecv.2021.12.003 . hal-03695493

HAL Id: hal-03695493

<https://hal.science/hal-03695493>

Submitted on 14 Jan 2024

HAL is a multi-disciplinary open access archive for the deposit and dissemination of scientific research documents, whether they are published or not. The documents may come from teaching and research institutions in France or abroad, or from public or private research centers.

L'archive ouverte pluridisciplinaire **HAL**, est destinée au dépôt et à la diffusion de documents scientifiques de niveau recherche, publiés ou non, émanant des établissements d'enseignement et de recherche français ou étrangers, des laboratoires publics ou privés.



Historical stained-glass window laser preservation: The heat accumulation challenge



Evan Maina Maingi^a, María Pilar Alonso^a, Luis Alberto Angurel^{b,*},
 Md Ashiqur Rahman^b, Rémy Chapoulié^c, Stéphan Dubernet^c,
 Germán Francisco de la Fuente^b

^a Área de Historia del Arte, Departamento de Historia, Geografía y Comunicación and Unidad Asociada de I+D+i al CSIC “VIMPAC”, Universidad de Burgos, P^o Comendadores S/N, 09001 Burgos, Spain

^b Instituto de Nanociencia y Materiales de Aragón, INMA (CSIC-University of Zaragoza), María de Luna 3, 50018 Zaragoza, Spain

^c Archéosciences Bordeaux laboratory UMR 6034, CNRS, Bordeaux Montaigne University, France

ARTICLE INFO

Article history:

Received 6 August 2021

Accepted 21 December 2021

Available online 3 January 2022

Keywords:

Conservation

Cultural heritage

Stained-glass

Heat accumulation

Ultra-short pulsed-laser

ABSTRACT

Stained-glass windows form an important part of cultural heritage. Short pulse lasers open new opportunities for safe decontamination. In this work, and for the first time, the interaction of sub-nanosecond and femtosecond pulsed lasers with some contemporary stained-glasses has been analyzed exploring their applicability to safely clean stained-glass windows. The results show that, in these materials, damage can be induced using energy levels below damage thresholds due to the heat accumulation in the coating layer that is being eliminated. The latter generates significant thermal stresses on the glass volume, which induce crack formation. In consequence, in order to apply safe stained-glass cleaning protocols, laser parameters have to be selected to control the temperature increase within this layer. To achieve the latter goal, two alternative irradiation procedures were explored in this work. As a first option, a reduction of the effective pulse repetition frequency to values lower than 20 kHz was applied. A second alternative was used for lasers with pulse repetition rates in the hundreds of kHz. In this case, the burst mode was employed controlling the number of pulses emitted and combined with an adequate time lapse selection between two consecutive burst runs. A proof of concept demonstration was carried out on a stained-glass sample from the Cathedral of Cuenca, dated at the end of the XV century.

© 2021 SECV. Published by Elsevier España, S.L.U. This is an open access article under the CC BY-NC-ND license (<http://creativecommons.org/licenses/by-nc-nd/4.0/>).

Conservación de vidrieras históricas con tecnologías láser: el reto de limitar la acumulación de calor

RESUMEN

Las vidrieras constituyen un elemento esencial de nuestro patrimonio cultural. Los láseres de pulsos ultracortos ofrecen nuevas oportunidades para desarrollar procesos de restauración seguros. En este trabajo, por primera vez, se estudia la interacción de láseres pulsados

Palabras clave:

Conservación

Patrimonio cultural

* Corresponding author.

E-mail address: angurel@unizar.es (L.A. Angurel).

<https://doi.org/10.1016/j.bsecv.2021.12.003>

0366-3175/© 2021 SECV. Published by Elsevier España, S.L.U. This is an open access article under the CC BY-NC-ND license (<http://creativecommons.org/licenses/by-nc-nd/4.0/>).

Vidrieras
Acumulación de calor
Láseres de pulsos ultracortos

emitiendo pulsos en el rango de los subnanosegundos y femtosegundos con piezas de vidrieras contemporáneas, con el fin de explorar la posibilidad de desarrollar procesos seguros de restauración de vidrieras. Los resultados muestran que, en estos materiales, incluso trabajando con niveles de energía por debajo de los umbrales de daño, se puede generar deterioro por la acumulación de calor generada en la capa que se está eliminando, lo cual puede generar niveles de tensiones térmicas que provocan la ruptura del vidrio. Por tanto, para desarrollar protocolos de limpieza seguros, los parámetros de procesamiento deben escogerse de tal manera que se minimice la temperatura que se alcanza en esta capa. Se han explorado dos alternativas. Una es reducir la frecuencia de trabajo hasta valores por debajo de los 20 kHz. En el caso de láseres que trabajen a frecuencias más elevadas, la alternativa es trabajar en modo *burst*, limitando el número de pulsos en cada serie y estableciendo tiempos de espera entre dos series. Estas ideas se han aplicado sobre una pieza de vidriera de la Catedral de Cuenca de finales del siglo XV.

© 2021 SECV. Publicado por Elsevier España, S.L.U. Este es un artículo Open Access bajo la licencia CC BY-NC-ND (<http://creativecommons.org/licenses/by-nc-nd/4.0/>).

Introduction

Glass was one of the most amazing materials in mediaeval buildings; it was technically, functionally and symbolically novel. Coloured glass pieces, carefully segmented, were assembled together in a lead frame to form what is referred to as stained-glass window. The artistic appearance of the glass would be enhanced by applying coloured paints, half-tones and/or dark contour lines [1–6]. Stained-glass has been put forth as one of the most delightful and compelling forms of decoration; notwithstanding, it is also one of the most vulnerable [7].

Stained-glasses have faced numerous deterioration phenomena over the centuries due to exposure to both human and environmental factors. The main types of degradation that affect them are those of physical, chemical and organic nature. Physical degradation includes abrasion, cracking, tearing, and exfoliation of surface layers among other phenomena that are not of chemical nature but which, if left unchecked, initiate and accelerate damage of chemical nature. Due to the thermal and mechanical properties of glass, temperature gradients can also induce crack generation [8]. This is more important in decorated glasses due to the additional stresses induced in the grisaille-glass boundary due to the lower thermal expansion coefficient values of grisaille in comparison with glass.

Chemical degradation is associated to the generation of corrosion, patina or mineral crust growth. Generally, the initial step of glass corrosion can be described as the attack of humidity on the surface. In all glasses, sodium and potassium oxides are hygroscopic [9]. Air pollutants, mainly CO₂ and SO_x, accelerate the above effect, leading to patina development and mineral crust growth over the glass surface, mainly associated to sulfates (gypsum and sunkenite) or calcite [10].

Deterioration can also be of organic nature, such as attacks by algae and lichens, for instance. Organic infestation creates soft deposits that attract and hold water on the surface, the consequent dampness can actively damage the glass. Acidic metabolic by-products from organic growth, can, over time, trigger corrosion damage even on post-mediaeval glass, further reducing its transparency [11]. Additionally, heavy traffic

and/or industrial pollution can deposit thick obstructing crust layers, which can be quite loose and flaky, but can also be extremely hard. Moreover, soot from decades of burning candles can gradually cause window glass to darken.

In general, one of the biggest challenges faced in conservation of historical stained-glasses and windows is the delicate removal of the accumulated crusts [12–14]. Stained-glass has been subjected to cleaning using mechanical (scalpels, bristle brushes or glass-fibre brushes) and chemical (water or organic solutions) methods. A number of surface coatings, paint interventions or consolidants have been proposed to restore and protect degraded paints that are found on stained-glasses [15]. The main limitation of these processes is that, the more effective the cleaning process is, the higher the possibility to damage the surface or to generate long-term damage [16,17]. For these reasons, additional alternatives were also explored, for instance, cleaning with luminescent ionic liquids [18] or the application of laser surface desorption methods [4,19].

The use of laser cleaning as a conservation technique in Cultural Heritage has been a subject of research for the last several decades [1,4,20–22]. Numerous studies have been published to date dedicated to broadening the knowledge in laser cleaning of various materials: metals [23–25], stones [26,27] or paints [28,29]. The absorption of laser radiation can lead to ablation. The latter involves the ejection of material from a laser irradiated surface, sometimes accompanied by the formation of plasma and shock waves, when intense laser irradiation is used [30]. The minimum energy density required to achieve ablation is called the ablation threshold. When the ablation threshold of the material to be removed is lower than that of the original substrate, the removal process can be performed within safe parameters. That is, the energy density deposited onto the sample surface is sufficient to clean the contaminants but not enough to damage the substrate material [31].

Laser cleaning has been investigated in the restoration of historical glass [32] and stained-glass windows [4,19,33–35]. As from the results of the project “Laser cleaning of stained-glass windows”, developed in Germany in the period 1997–2000 [4], an excimer laser operating at 248 nm with pulse durations in the range 20–40 ns and a pulse repetition frequency

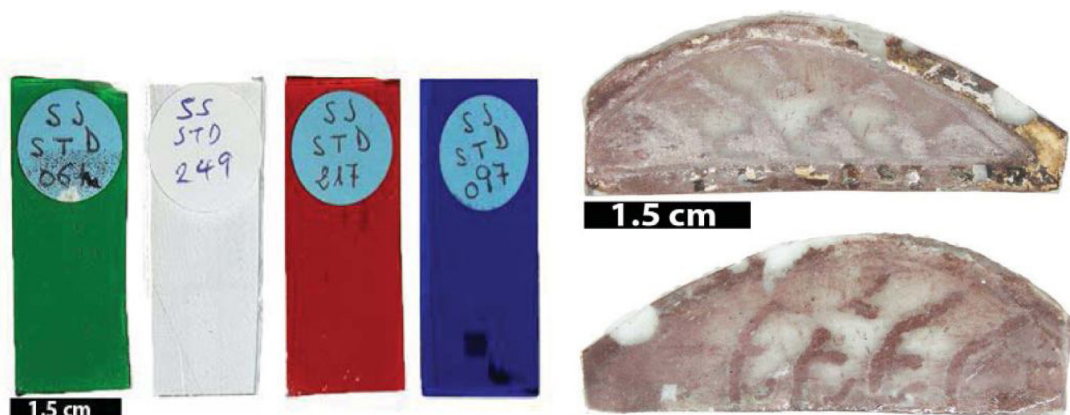


Fig. 1 – Photographs of the green, colourless, red and blue glass samples used in this study (left). Front and verso sides of the historic glass piece from the Cuenca Cathedral (right).

of 50 Hz was selected. It enabled cleaning of different dense crusts, bio- and organic coatings with low thermal loads. In addition, the performance of a 248 nm excimer laser was compared with other lasers with different wavelengths: 193, 308, 355 and 1064 nm and pulse durations in the range between 5 and 30 ns [32]. In all the cases, pulse repetition frequency was in the order of 1–4 Hz. In these studies, it was observed that the Nd:YAG ($\lambda = 1064$ nm) laser was not adequate because the observed temperature rise was too high and caused deterioration of the glass. In the case of the third harmonic of the Nd:YAG ($\lambda = 355$ nm), some solarization effects (discoloration inside the glass), mainly associated with MnO_2 photo-oxidation [12], were observed. This effect was reversible if the sample was heated. With the other wavelengths, alteration and ablation threshold values were very low, reducing the range of cleaning laser parameters that can be used in the restoration of the glass. Depending on the glass optical properties and the thickness of the layer to be removed, it is also possible to develop cleaning protocols using laser incidence from the opposite side [36]. Laser treatments can be combined with photoacoustic measurements in order to determine the ablation threshold.

Laser technology has evolved very fast during the last few decades and new ultra-short pulsed lasers are now commercially available. These open new opportunities for laser cleaning in Cultural Heritage restoration. Pulse durations can be modified in the range of fs and ps with pulse repetition frequencies that can be selected from few kHz to MHz. The short pulse duration reduces the level of heat generation and allows a greater control of the layer thickness that is affected by the laser. In addition, the available repetition frequencies are high enough to accomplish efficient cleaning speeds. However, they also increase heat generation when incident energy is absorbed [37–40]. This is especially relevant when laser treatments are applied in the processing of glasses, where thermomechanical stresses easily deteriorate the material.

In this work, the interaction of ultrashort ps and fs pulsed lasers has been explored in contemporary stained-glass samples, frequently used in restoration interventions, with two main objectives. The first one is to increase the understanding of the phenomena that take place during laser cleaning of

these materials. The second one is to establish a relationship between laser irradiation parameters and the damage caused on the glass during laser intervention, in order to enable the definition of a safe cleaning procedure. This has been initially studied in some contemporary stained-glass samples that were painted with permanent ink. Cleaning protocols to remove the ink from the glass surface without inducing defects on the sample surface were defined for lasers with very different specifications. Recently developed ultra-short pulse lasers provide a range of emission parameters which include very high pulse frequency values which, in turn, would reduce the required time for cleaning a given surface. Limits associated with the use of such high pulse frequency values have also been analyzed, however, in order to avoid heat accumulation and associated damage to the glass substrate. Finally, the ideas that were extracted from experiments with modern glasses have been applied to laser cleaning of a colourless historic stained-glass window sample from the Cathedral of Cuenca (Spain). The latter was fabricated at the end of the XV century and it exhibited a similar behaviour to the modern glass samples, in spite of their historical and technological differences.

Materials and methods

Stained-glass samples

Four contemporary stained-glass samples of different colours (green, colourless, red and blue) were selected for this study (Fig. 1). These samples were supplied by the glass factory of Verreire de Saint-Just, located in Saint-Just-Saint-Rambert, in Loire (France). This factory was founded about 189 years ago. Currently, Verreire de Saint-Just glass maker is a reference supplier of glass and stained-glass in Europe. The samples have a rectangular shape with dimensions $4 \text{ cm} \times 1.5 \text{ cm} \times 2 \text{ mm}$. Elemental chemical compositions were determined by EDS analyses and are presented in Table 1. The major components found in the green, colourless and blue glasses include SiO_2 , Na_2O , CaO , and MgO . Differences in colours are reflected in the presence of small amounts of other elements, as for

Table 1 – EDS elemental analyses (at%, acquisition time 500 s) obtained on the four contemporary glasses and on the historic stained-glass sample subjected to study in this work.

Glass	O	Si	Na	Ca	Mg	K	Al	Cr	Cu	As	Zn	Ba	Cl
Green	57.8	25.2	12.3	3.3	1.0	0.1		0.1	0.1				
Colourless	58.3	25.5	11.7	3.3	0.9		0.2			0.2			
Red	58.3	25.6	11.5	3.4	1.0	0.1	0.2			0.2			
Red, surface	57.7	27.1	7.0			5.6					2.1	0.5	
Blue	57.8	25.1	12.6	3.4	1.0								
Historic glass	57.9	23.4	6.0	4.5	2.5	3.5	1.8						0.4

instance Cr and Cu in the green glass. The red glass differs from the above. In this case, the glass exhibits an external layer of 267 μm with a different composition. Its bulk composition is similar to that of the other glasses, but its external layer includes SiO_2 , Na_2O and K_2O as main components, as well as important amounts of Zn and Ba.

This study also involves laser cleaning of a decorated historic stained-glass sample from the Cuenca Cathedral in Spain. It is irregularly shaped and has reddish-brown paintings on its surface, with remnants of putty along the edges. Its dimensions are approximately 4.8 cm \times 2 cm \times 2 mm (Fig. 1). The composition of this glass is also presented in Table 1, showing higher amounts of Ca, Mg, Al and K compounds in comparison with the modern stained-glass samples. It is also important to note that the Na content is lower for this historic sample.

Lasers used in the cleaning protocols herein reported

Laser treatments were performed using two different lasers. A picosecond (ps) near-infrared laser (PowerLine Pico 10-1064, Rofin-Sinar, Germany) with a wavelength of 1064 nm, a pulse duration of 800 ps and a maximum output power of 8 W, coupled with a galvanometer mirror system. The pulse repetition rate can be modified between 250 and 800 kHz and the waist diameter of the laser beam ($1/e^2$ criterion) is approximately 80 μm , as deduced following the D^2 -method proposed by Liu [41].

Treatments were also carried out using a femtosecond (fs) laser (Carbide model, Light Conversion, Lithuania), also coupled to a galvanometer mirror system (Direct Machining Control, UAB, Vilnius, Lithuania). Treatments were performed in this case at 1030 nm, with a pulse duration of 228 fs, a maximum output power of 40 W and a beam diameter of 100 μm . Pulse frequency can be modified between 1 kHz and 1 MHz and the system offers the possibility of selecting the final frequency using the pulse peak divider option.

Laser scanning was performed in two different modes: beam scan and burst. In the beam scan mode, the laser scans the surface at a given speed, controlling also the distance between two consecutive scan lines. The burst mode consists on a spot-by-spot scanning process with adjustable laser parameters. The laser system produces a sequence of a defined number of pulses (a burst) controlling the repetition rate [30]. A single burst is incident at a given position and the distance between the positions, the number of pulses in a burst, as well as the energy of each individual pulse can all be set by software. This surface scanning process is slower than the continuous one because the laser stops at every point. In

the case of the n-IR ps laser, all the treatments were performed in the burst mode in 2 mm \times 2 mm regions, with a distance between burst spots of 200 μm in order to reduce heat accumulation. When the femtosecond laser was used, the distance between burst pulse spots was maintained with an overlapping of 90% or 70% of the beam diameter, in order to open the possibility to uniformly clean a given area in a single step process.

On the contemporary glass samples, these laser treatments were applied directly to the glass surface or to clean a graffiti purposely generated on the glass surface. Some areas of the samples were painted with blue permanent ink (Staedtler Lumocolor permanent marker) in order to ascertain their effect on laser cleaning protocols. The ink is an alcohol (propanol, ethyl alcohol) based compound with a resin-based binding agent. These experiments were designed to analyze the phenomenology that appears while this external coating is being eliminated with the laser treatment.

Furthermore, the glass average temperature increase was recorded using a thermal camera (Thermo Cam P25, Teledyne FLIR Systems, USA) during representative laser treatments. Spatial and temporal resolution of the thermal camera have to be considered because it provides an average temperature reading. During a very short time span, the temperature that can be reached at the laser focal spot on the surface of the glass can be much higher. It is very localized, however, and the interaction time is insufficient to appreciably elevate the glass temperature [42]. In contrast, the temperature reached on the glass bulk, below the layer being desorbed during laser cleaning, will be very close to the average temperature measured with the thermal camera, providing a reliable reference to avoid damage.

Optical and surface characterization

The differences in colour between the glasses suggest that they can exhibit different absorption properties at the emission wavelength of the laser. The transmittance and absorption values in the UV–Vis–nIR range, in particular between 300 and 1100 nm, were characterized using a StellarNET Miniature Spectrometer. A SL1-CAL light source, 0.6 mm in diameter and a cone angle of 25.4° at the output of the optical fibre and specifically configured for irradiance calibrations in the 300–1100 nm range, was used. Transmittance tests were carried out with an integration time of 5 ms, averaging 100 scans.

Transmittance measurements were also performed using the processing lasers with power levels similar to those used in the cleaning experiments. For a given nominal power the

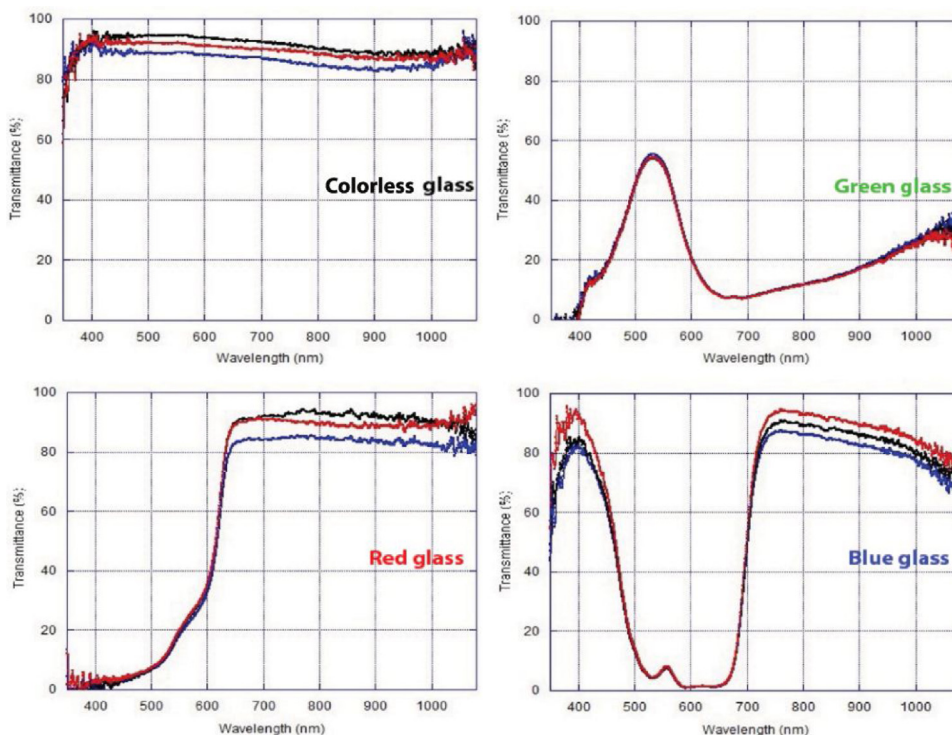


Fig. 2 – UV-Vis-NIR transmittance spectra recorded for three separate samples of each of the four contemporary glasses subjected to study in this work.

laser reaches a thermopile power sensor (LM10 Coherent), first directly and, in a second run, through the glass that was being characterized.

Optical characterization was also completed by observing the response of the samples to UV radiation generated by a UV laser (PowerLine Pico, Rofin-Sinar, Germany) with a wavelength of 355 nm, a pulse duration of 300 ps and a maximum output power of 3 W coupled with a galvanometer mirror system. The pulse repetition rate can be modified between 250 and 800 kHz. The laser beam has an elliptical shape and the laser beam waist axes dimensions ($1/e^2$ criterium) are approximately 34 and 29 μm .

Sample surfaces were observed before and after the laser treatment with a JSM 6360-LV Scanning Electron Microscope (SEM). Images were taken in a vacuum mode at 20 Pa. Polished transverse samples were also analyzed using a Field Emission Scanning Electron Microscope (FE-SEM, Carl Zeiss MERLIN). Semiquantitative elemental analysis of the glass samples was performed using Energy Dispersive X-ray Spectroscopy (EDS, INCA350, Oxford Instruments) with acquisition times of 500 s. These observations were completed with optical microscopy photographs. Topography of the surface after laser cleaning was measured using a confocal microscope (Sensofar PL μ 2300).

Results and discussion

Laser interaction in contemporary glasses

Initial experiments were performed in the set of contemporary glasses described. Differences in their optical properties were

initially evaluated, observing that the green glass exhibits a different behaviour with respect to IR radiation when compared to the other coloured contemporary glass samples. Laser cleaning protocols, considering the characteristics of the two IR laser systems that have been used in this work, were explored in order to identify the limiting factors for a safe cleaning protocol.

Analysis of optical properties

Fig. 2 shows the transmittance spectra corresponding to the different types of contemporary glasses studied. For each sample, spectra were acquired in three different positions, in order to obtain information about the homogeneity of the optical response in each glass. In all the cases, differences lower than 10% are only observed in the regions of the spectra with transmittance values higher than a 70%. These differences have been associated to the distribution of micro-bubbles inside the glass in the illuminated (approximately 1 cm in diameter) areas.

As expected, the differences in colours generate very different transmittance spectra. For example, in the spectral range close to 1064 nm colourless, red and blue glasses absorb less than 20%. The amount of energy that is absorbed by the green glass, however, increases to values approaching 70%. In the region of the spectrum close to 530 nm, corresponding to the emission of green lasers, it is also observed that the amount of absorbed energy is very high in the three coloured glasses and only the colourless one presents high transmittance values. Finally, the four glasses, in particular the green and red one, exhibit lower transmittance values in the proximity of 355 nm,

Table 2 – Transmittance values obtained with a laser power metre, directly or through the different glass samples used for this study employing near-IR and UV laser sources with the specified emission.

	n-IR laser $\lambda = 1064 \text{ nm}$, $\tau = 800 \text{ ps}$		UV laser $\lambda = 355 \text{ nm}$, $\tau = 300 \text{ ps}$	
	Recorded power (W)	% transmittance	Recorded power (W)	% transmittance
Direct incidence	2.35	–	0.29	–
Colourless	2.05	87	0.15	52
Green	0.76	32	0	0
Red	2.01	86	0	0
Blue	1.72	73	0.13	45

a characteristic emission wavelength for third harmonic (UV) solid state and rare-earth fibre lasers.

These experiments were performed with a light source in which the irradiance level (power density) is very low. In order to check if this behaviour is similar when the direct laser radiation is used, a set-up was built in which the energy that reaches a thermopile power sensor is recorded when the laser is focused directly on it (direct incidence), or through each one of the different glasses. Table 2 collects the transmittance values measured for each sample, using the 800 ps n-IR laser, with a fluence value of 0.06 J/cm^2 and an irradiance level of 74 MW/cm^2 , and the 300 ps UV laser (fluence 0.01 J/cm^2 , irradiance 33 MW/cm^2) as emitter sources. Results presented in Table 2 and in Fig. 2 correlate very well, confirming that both types of measurements are equivalent for these materials.

The above results seem to indicate that laser treatments on colourless, blue and red stained-glass windows using IR radiation can be safer than using UV radiation because, once the IR laser radiation reaches the glass sample, the percentage of transmitted radiation is higher. But IR radiation effects have a strong thermal component and, in consequence, if absorbed, the sample temperature increases locally, inducing thermo-mechanical stresses that can generate micro-cracks in the sample. Due to this fact, the response of the green glass to IR radiation is expected to be different.

The laser power metre used in these experiments determines the laser power by measuring the temperature at its sensor. From this measurement, the temperature evolution at the surface of the sensor is observed to reach a stable value after several seconds. Within this time frame, the higher absorption values observed in the green glass led to further heating and higher temperature gradients between the incident laser spot and its surroundings. This led to the fracture of the green sample during these optical transmittance studies when the IR laser radiation was used.

Analysis of damage generation during laser cleaning with an 800 ps high pulse frequency system

Due to the high pulse repetition frequencies that are available in this laser system, the overlap between consecutive pulses is important in the cleaning protocols that can be applied with this laser. In order to separate the contributions of the temporal and spatial overlap with this system, the burst mode configuration was selected. The laser treatment was initially applied directly on the glass surface, in order to define a damage threshold. It was observed that the damage threshold was above the maximum fluence and irradiance levels that could be reached with this laser. These are reached by selecting high

power and low frequency values, resulting in a pulse energy value of $24 \mu\text{J}$ (fluence 0.49 J/cm^2 , irradiance 0.61 GW/cm^2).

Treatments were applied in areas of $2 \times 2 \text{ mm}^2$ and with a distance between spots of $200 \mu\text{m}$ in order to study the effect of the temporal overlap in each position. Different experiments were performed increasing the number of pulses in each position in steps of 200. In the case of the colourless, blue and red glasses, no interaction with the glass surface could be observed, even if the number of pulses in each position increased up to 10,000. The phenomenology observed in the green glass is different. This material exhibits the highest absorption coefficient at this wavelength, as expected from its experimentally determined transmittance value using a laser source (Table 2). An increase of the temperature at the glass surface during laser treatment is consequently expected. Fig. 3(a) shows this evolution in case of red and green glasses for one series of 200 pulses and after having repeated the laser treatment 5 times. The time required to treat this area with these processing parameters is approximately 0.42 s. Table 3 also shows the maximum temperature increment measured during these experiments. Measured values reach $\Delta T = 3.9^\circ\text{C}$ for the red glass after 5 series of 200 pulses in each position. In contrast, values of 35.9°C (200 pulses) and 100.9°C (5×200 pulses) were reached for the green glass under similar irradiation conditions. An appreciable degree of damage can be observed on the surface of this last sample after having applied a series of 2000 pulses in each position. The level of damage increases with an increase in the number of pulses. Fig. 3(b) shows the damage induced by laser irradiation after 5000 pulses in each position. Fig. 3(c) and (d) shows the topography and a profile in a line. Laser scans were carried out in the vertical direction, moving from left to right in the image. The level of damage also evolves following the geometry described by the laser scanning. This fact indicates that damage is not directly related with the level of energy that is applied in each position. In contrast, due to heat accumulation, the temperature of the glass increases while the laser treatment evolves, increasing also the level of thermomechanical stress that can induce glass failure [43].

Similar studies were performed during cleaning protocols, covering selected glass surface areas with blue permanent ink. The following experiments were performed with the objective of removing this ink from the glass surface, as well as to observe the after-cleaning effect on the substrate using the same irradiance levels. It is important to mention that the coating layer was not uniform, with thickness values ranging between 450 nm and $1.6 \mu\text{m}$. Irradiation experiments were initially performed on the colourless, blue and red glasses. Evi-

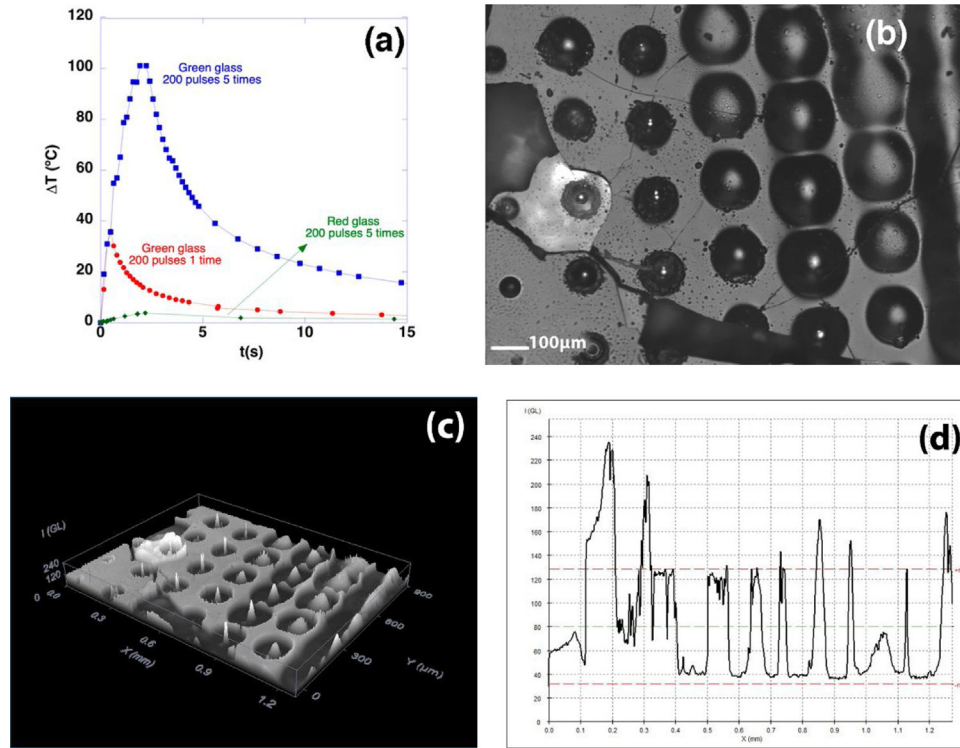


Fig. 3 – (a) Temperature increase recorded with a thermal camera for approximately 30 s on the glass surface during several laser treatments (series of 200 pulses in each position) performed on the green and red glasses. (b) SEM micrograph of the surface of the green glass after direct laser irradiation with 5000 pulses in each position. The distance between two positions is 200 μm . The laser scans in the vertical direction of the image, starting on its left lower corner and showing that the damage level increases while the laser treatment evolves. (c, d) Isometric display and profilometry of the treated area.

Table 3 – Maximum temperature increments reached on the surface of the green and red glasses after several laser irradiation treatments in which successive bursts with 200 laser pulses were applied in each position.

	Green glass		Red glass	
	200 pulses once	200 pulses 5 times	200 pulses once	200 pulses 5 times
Without ink	35.9 °C	100.9 °C	1.1 °C	3.9 °C
With ink	81.9 °C	–	9.3 °C	21.0 °C

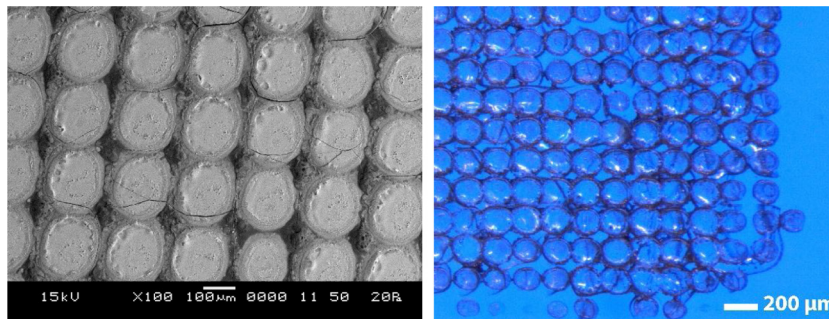


Fig. 4 – SEM micrograph (left) and photograph (right) of the ink-coated blue contemporary glass sample after laser irradiation with 500 pulses in each position.

dence of laser interaction with the ink coating was observed after 200 pulses, when the thinnest regions of the ink were removed from the glass surfaces. After this laser treatment, the sample surface did not present any apparent damage,

demonstrating that these laser emission parameters do not cause critical photo-thermal stress in the irradiated glass. In contrast, when the number of pulses in each position is increased to 500 (Fig. 4 for blue glass), the cleaning process

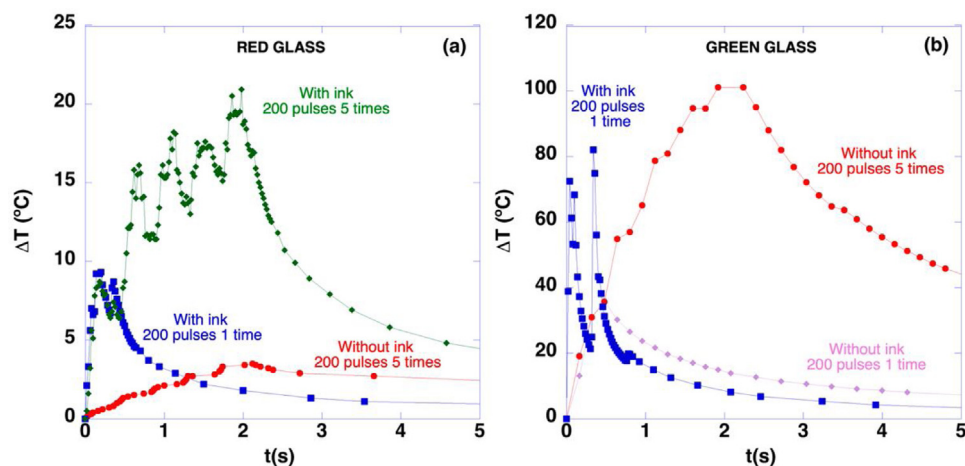


Fig. 5 – Comparison of the average maximum temperature increment reached in the glass measured with a thermal camera during laser cleaning processes in the (a) red and (b) green contemporary glasses with and without the ink coating.

generates a large number of visible defects on the glass. These are observed even if the number of applied pulses is an order of magnitude lower than those applied to the uncoated glasses without affecting their surface. A closer look at the detail of the marks observed in the coating suggests that pulsed laser irradiation has induced melting of the ink. Moreover, it seems that significant heat transfer takes place from the coating to the glass underneath, increasing the temperature at the glass surface. Consequently, the associated thermo-mechanical stress leads to the observed micro-crack formation on the glass substrate.

These experiments show that the damage in the glass is not caused by the direct laser-glass interaction. Cracks are generated by heat accumulation in the coating, which generates a significant local temperature gradient on the glass surface and induces thermo-mechanical stresses above the fracture limit of the material. In consequence, the laser parameters have to be defined in order to control this heat accumulation.

As experiments were initially performed with pulse frequency values close to the lowest ones allowed in this system, additional experiments were performed maintaining series of 200 pulses and repeating these series several times. In this configuration, the laser applies 200 pulses in a given position during 0.67 ms and subsequently moves to the adjacent position. Once it has covered the desired area (in this case 0.42 s for a single series covering an area of 2 mm × 2 mm), the process is repeated again for the desired number of times. Fig. 5 shows how average temperature has increased in the sample surface of the red and green glasses after several of these treatments, where the laser protocol has been repeated once or five times. The increment in the temperature (see Table 3) is clearly higher when the laser treatment is applied to remove the ink layer than when the same laser treatment is performed directly over the noncoated glass surface. Fig. 6 shows the evolution of an ink-coated colourless glass surface after irradiation with several series of 200 laser pulses. Fig. 6(a) and (b) shows the aspect after the first series. The ink starts to melt mainly in the centre of the spot, due to the Gaussian energy distribution within the laser beam cross-section, but

it is not removed from the glass surface. The size of the area affected by the laser spot depends on the thickness of the original coating. In the thinnest regions (left column in Fig. 6(a)) the diameter of these affected areas is smaller than 50 μm (left column in Fig. 6(a)); in the thickest regions, the diameter of the spot left by the laser increases up to approximately 200 μm. After cleaning the ink with alcohol, the glass surface did not exhibit any visible damage.

When the number of series increases up to 5, equivalent to a total of 1000 pulses (Fig. 6(c)), it is possible to eliminate the ink layer over the glass surface in the centre of each spot, where the energy is maximum. This area is surrounded by a region that has been affected by temperature increases in the ink layer. There is some evidence of damage of the glass surface, however, mainly observed in the centre of the spot after having removed the rest of ink over the glass surface (Fig. 6(d)). This level of damage is not the same in all the spots, and apparently depends on the uniformity of the ink layer thickness. This reflects the difficulty of working with a coating thickness that is not uniform. This situation is common in historical stained-glasses, where non-uniform grisaille and crust layers are usually found.

When the number of series increases to 10, removal of the coating is observed more easily at the centre of the spot (Fig. 6(e)). As in previous cases, some defects are observed on the glass surface after cleaning (Fig. 6(f)), mainly located in sections where the coating is thicker. Topographies of these regions with defects are presented in Fig. 6(g) and (h).

Comparing the levels of damage presented in Fig. 4 (500 pulses in each position) and Fig. 6 (10 series of 200 pulses), it is observed that it is possible to apply 2000 pulses on top of the coating generating a lower number of cracks on the glass, as long as a sufficient time lapse between pulse bursts is applied.

Subsequently, it is important to have an additional reduction in the heat generated during the laser treatment. This reduction is achieved by increasing the time lapse between two series of pulse bursts up to several seconds. From the analysis of the dependence presented in Fig. 3(a), a time lapse of approximately 26 s is needed to reduce ΔT generated in one

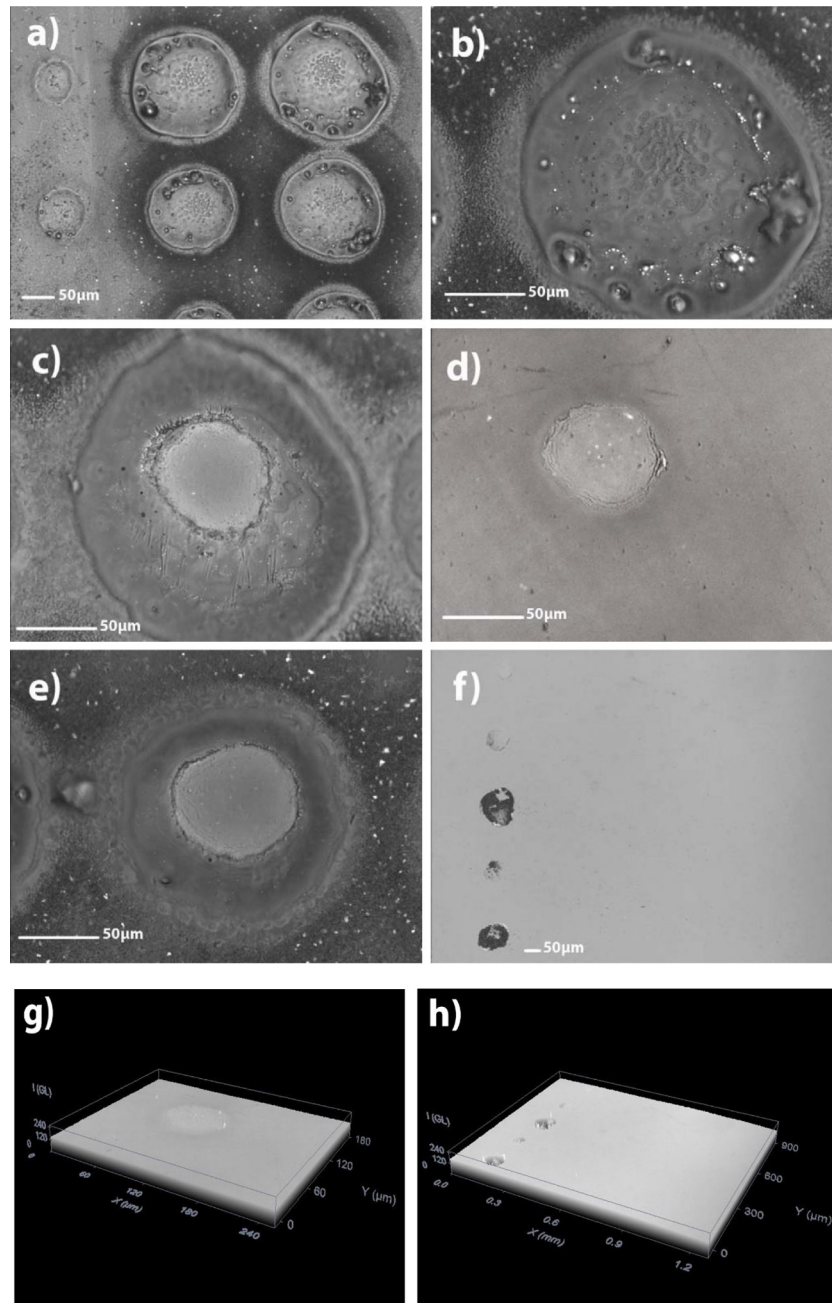


Fig. 6 – Optical micrographs of the surface of the ink-coated colourless glass after irradiation with one (a and b), five (c and d) and 10 (e and f) series of 200 pulses. (d) and (f) show the aspect of the glass surface after conventionally removing the remaining ink on the glass surface, once the laser treatment was completed. Several defects generated during the laser treatment are thus revealed. Figures g and h show isometric aspects of (d) and (f).

series to values lower than 1°C . Fig. 7 shows representative optical micrographs of the marks generated by the laser in different sections of the ink-coated red glass sample with a lapse time of 30 s between two series. As in previous experiments, the laser covers an area of $2\text{ mm} \times 2\text{ mm}$, marking a point every $200\ \mu\text{m}$ and applying 200 pulses in each position. Fig. 7(a) and (b) correspond to a situation in which five series of 200 dots were applied. The time lapse between two series allows a more effective cooling of the glass between the laser treatments and reduces the heat accumulation level.

Obviously, with this laser protocol, the coating thickness removed in each series is reduced but the laser treatments are safer for the glass integrity. Fig. 7(b) shows that this initial treatment was not sufficient to remove completely the coating in some regions, though selective removal was observed as in the previous experiments.

Fig. 7(c) and (d) shows also the aspect of the surface after applying 10 series of 200 pulses. The coating on the surface of the red glass (centre of the spot) was removed with no observable damage to the substrate. This is also clearly observed in

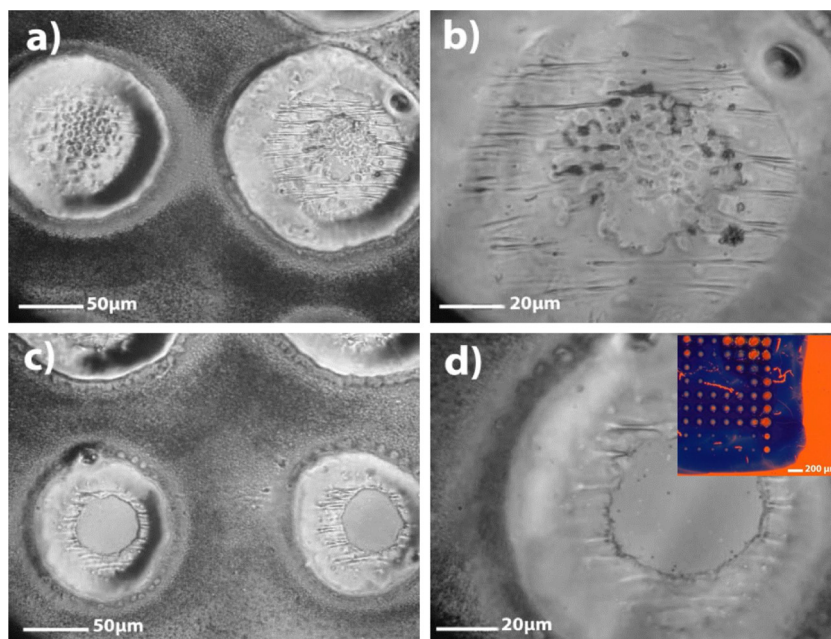


Fig. 7 – Optical micrographs of the red glass surface irradiated with five (a and b) and 10 (c and d) series of 200 laser pulses. A 30 s time lapse between two consecutive series of pulses was applied. The inset corresponds to a photograph of the red glass surface after the laser treatment.

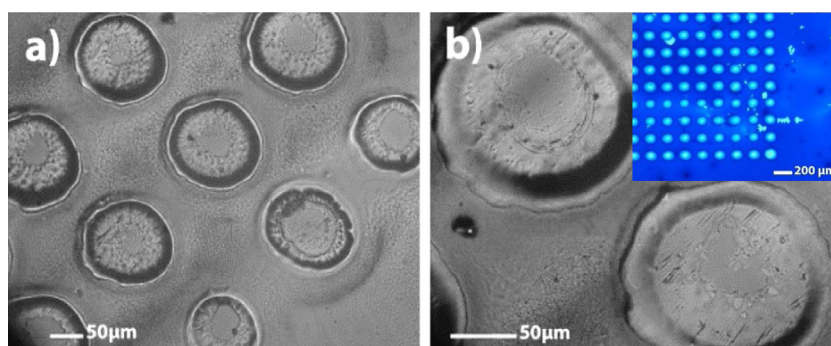


Fig. 8 – Optical micrographs (a and b) of the green glass surface irradiated with ten series of 200 pulses and a time lapse of 30 s between two consecutive series of pulses. The inset corresponds to a photograph of the green glass surface after the laser treatment.

the inset of Fig. 7(d). After completely removing the ink layer, no substrate alteration was observed on the glass. In this case, the cleaning threshold was achieved by using a given set of minimum number of pulses per treated area, combined with short intervals between each exposure.

This laser protocol has also been applied to the ink-coated green glass surfaces. Fig. 8 shows that the coating can be removed from the sample surface also in this glass, applying 10 series of 200 pulses. Comparing Fig. 8 with Fig. 4 it can be deduced that, maintaining the number of pulses at 200 and irradiating 10 times with the corresponding time-lapse intervals resulted in an acceptable removal of the surface coating with no damage to the substrate.

The proposed cleaning protocol generates a square lattice of cleaned spots. In order to cover the full area, the protocol can be repeated by moving the lattice subsequently a given fraction of the cleaned footprint. Once a full set of lines have

been cleaned, the process can be repeated in the perpendicular direction to achieve a completely cleaned surface.

Analysis of damage generation during laser cleaning with a fs system

Following the ideas deduced from the previous experiments, additional studies were performed with a femtosecond IR laser system using the beam scanning protocol. In this case, as lower pulse repetition frequencies are available, it is possible to control heat accumulation by reducing the effective pulse repetition frequency. Weber et al. [40] calculated the maximum temperature reached during laser treatment and determined that this temperature increases with the pulse laser frequency and is particularly dependent on the material's properties. Using the IR fs laser, the experiments were performed by selecting high power (40 W) and a basic frequency value of 200 kHz, giving a pulse energy value of 200 μJ

Table 4 – Cleaning parameters applied on the contemporary colourless glass using the fs IR laser. In all cases overlap between consecutive pulses or lines is 90% of the beam diameter.

Treatment	Frequency (kHz)	Laser speed (mm/s)	Distance between lines (μm)	No. of times	Observations
T1	40	400	10	2	Plain glass with no ink. No effect.
T2	40	400	10	2	Ink removed. Cracks observed on the substrate.
T3	20	200	10	1	Ink removed. No cracks.
T4	20	200	10	2	Ink removed. No cracks.

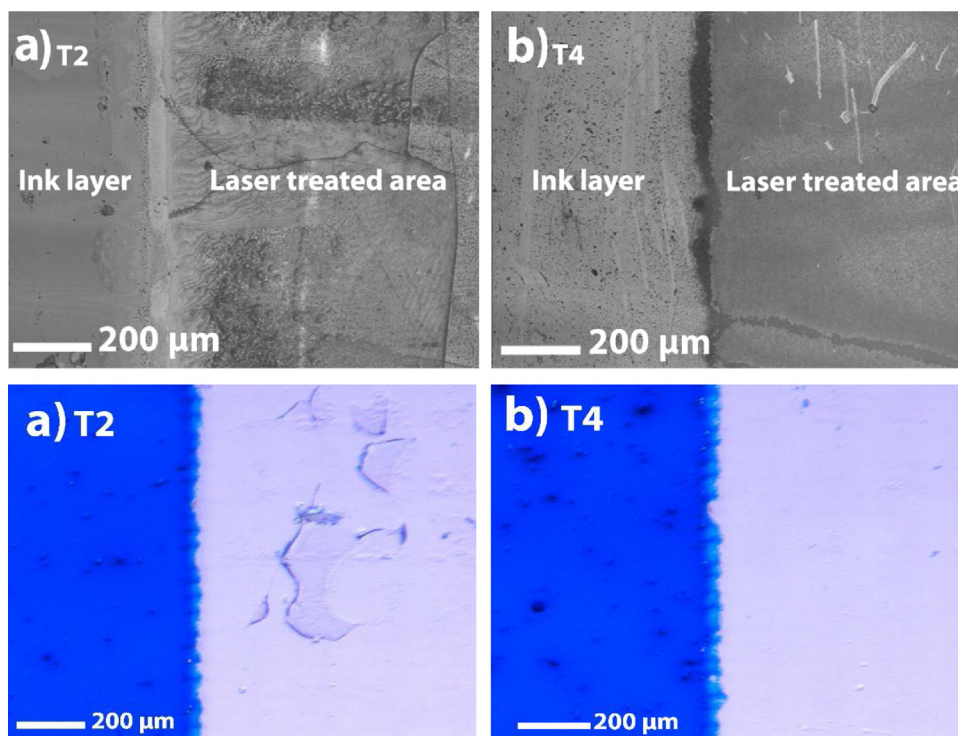


Fig. 9 – Optical micrographs (top) and photographs (bottom) of the contemporary colourless glass surface after two different laser cleaning protocols were carried out using (a) 2 series of 200 pulses at 40 kHz as described in treatments T2 and (b) 2 series of 200 pulses at 20 kHz as detailed in T4.

($2.55\text{ J}/\text{cm}^2$, $10^4\text{ GW}/\text{cm}^2$, 5000 times higher than the value reached with the 800 ps laser). Using the Pulse Peak Divider option, it was possible to select the effective frequency, and, in consequence, the time between two consecutive pulses, maintaining the pulse energy value constant. As can be observed in Table 4, effective frequency and scanning laser speed values were initially selected maintaining a distance of $10\ \mu\text{m}$ (overlapping of a 90% of the beam radius) between spots. The same value was selected for the distance between two scanning lines in order to maintain similar overlapping in both scan directions. Some experiments were repeated twice, rotating the second treatment by 90° .

Treatment T1 was applied directly on the glass and it was observed that even with the higher pulse repetition frequency selected in these experiments, the energy absorption was low during the laser treatment and no damage was observed on the glass. In contrast, when a laser treatment with the same laser parameters was applied in a region that was covered with ink (T2), it was observed that heat accumulated in the

ink induced thermal stresses on the glass substrate. These led to the appearance of cracks on its surface, as can be observed in Fig. 9(a). In order to reduce heat accumulation, the same cleaning experiment was performed reducing the effective frequency to 20 kHz. The scanning speed was also reduced to 200 mm/s to maintain the overlapping percentage and the spatial energy distribution. This approach increases the time between two consecutive pulses, reducing the maximum temperature reached in the coating to be eliminated. As can be observed in Table 4 (treatments T3 and T4) and in Fig. 9(b), ink was removed from the glass surface without generating cracks.

Experiments performed on contemporary stained-glass clearly indicated that in the development of safe laser cleaning procedures, an essential limiting factor is the maximum temperature that can be reached on the glass surface while the coating is being removed. In particular, when glass is highly transparent to the laser irradiation employed, defects in the glass are caused not by direct laser-glass interaction, but by

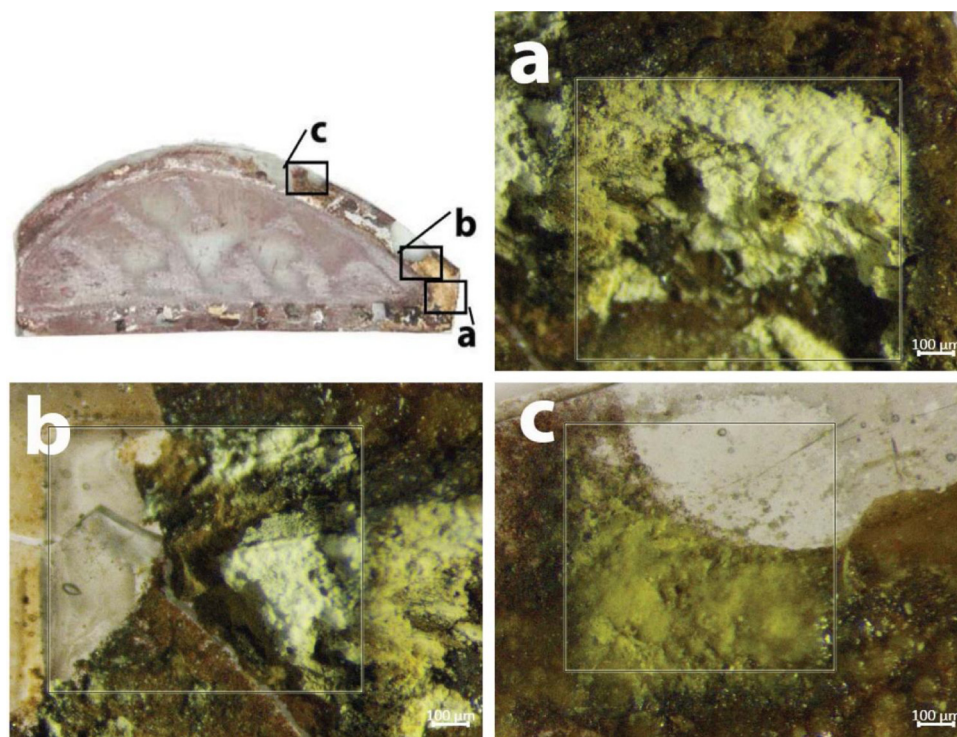


Fig. 10 – Optical micrographs of the mediaeval decorated glass surface after cleaning using a fs IR laser. The treated areas are marked with a square. Note the colour change from dark brown (untreated surface) to whitish-brown (treated surface).

Table 5 – Cleaning parameters applied on the historic colourless glass using the fs IR laser. In regions a and b the overlap between consecutive pulses or lines is 90% of the beam diameter, while this is reduced to 70% in region c.

Treated region	Frequency (kHz)	Laser speed (mm/s)	Distance between lines (μm)	No. of times	Observations
a	20	200	10	2	Cleaning achieved.
b	40	400	10	1	Cleaning achieved. Micro-cracks generated.
c	10	300	30	20	Cleaning achieved.

the thermal stresses associated with the heat accumulated within the absorbing deposits or contaminants on its surface.

Application to laser cleaning of historic glass

Following the same criteria, new experiments using the fs laser were applied on a colourless mediaeval stained-glass sample from the Cathedral of Cuenca (Spain). The glass exhibits a patina of gypsum ($\text{O/S/Ca} = 3.5/1/0.8$ in at%) over the full area and also putty is present in the border of the piece. Results after three laser treatments on the areas covered by the putty are presented in Fig. 10. Cleaned areas have been marked with a square. The detail of the laser parameters used in each of the treatments are indicated in Table 5.

Initial experiments were carried out on this sample in order to check possible damage to the glass when irradiation takes place directly on its surface. With the levels of irradiance reached with this fs laser (10^4 GW/cm^2), no damage was detected. Cleaning treatments were thus applied in the three regions shown in Fig. 10, where putty was covering the glass.

In the two initial regions, the importance of heat accumulation was also checked. Treatment in region a was the

same as that of T4 in the contemporary glass, maintaining the effective pulse frequency at 20 kHz and keeping a distance between laser pulse spots of $10 \mu\text{m}$ in both scan directions. As is observed in Fig. 10(a) this treatment was able to eliminate the upper brown layer of the putty. Below this upper layer, a white layer was revealed and the efficiency of the IR radiation for removing this material decreased. In region b, the frequency was increased to 40 kHz, reaching the conditions similar to those of treatment T2 that induced cracks in the contemporary glass, and also a crack was observed in the mediaeval glass. On the top left part of the cleaned area in Fig. 10(b), a gypsum layer was present on top of the glass. Laser treatment can eliminate completely this layer without inducing thermal damage on the glass. By contrast, when laser treatment is applied in a region containing putty (right part of the image) a crack is observed.

In region c, the applied laser treatment was less intense, the frequency was reduced to 10 kHz and the laser scanning speed was increased up to 300 mm/s, increasing also the distance between pulse spots up to $30 \mu\text{m}$ (overlapping of a 70% of the beam diameter). The process was repeated 20 times and no damage was observed on the sample. When the laser irradi-

ation reached the glass surface directly (upper right corner of the treated area), the gypsum layer was removed without deteriorating the glass. The putty layer started to be affected by the laser. In consequence, the laser treatment could be repeated several times without affecting the glass surface while eliminating the putty.

Conclusions

This work demonstrates that when IR laser cleaning is applied to remove contaminating layers from the surface of a glass, the limiting factor is the control of the maximum temperature reached within the outermost layer, even if the levels of the applied laser irradiance or fluence values are lower than those specified for the glass damage threshold. Several experiments have shown that laser treatments that do not cause any direct damage to the glass, deteriorate it if they are applied to remove contaminants that are deposited on the glass surface. The heat generated on the contaminant material to be cleaned induces a level of thermal stress which is high enough to cause mechanical cracks on the glass. In consequence, one of the main objectives of an ideal set of laser parameters to establish an effective cleaning protocol is to minimize this heat input, referred in this case as heat accumulation.

When high frequency burst laser treatments are applied, the temperature reached is limited by selecting a maximum number of pulses at each position of the burst series and introducing a time lapse between each series. In the particular case of the n-IR 800 ps laser used in this work, pulses of 24 μ J (Fluence 0.49 J/cm² and Irradiance 0.61 GW/cm²) in treatments with 200 pulses for 10 cycles or more, with non-irradiation time-lapse intervals between each treatment, resulted in a more observable and effective cleaning. This was also proved to be effective at avoiding micro-cracks and melting in the substrate, even if the glass shows an important level of absorption.

On the other hand, some new lasers have the possibility of reducing effective pulse repetition frequency while maintaining the energy per pulse. In this case, the reduction of such frequency is sufficient to define safe cleaning protocols, even if scanning speeds are also reduced to maintain a desired pulse overlap. This was demonstrated in the present work using a fs laser-based treatment which provided irradiance values in the proximity of 10⁴ GW/cm². Safe laser treatments have thus been achieved limiting the pulse repetition frequency to 20 kHz or below.

These ideas are also essential in designing laser protocols that avoid glass damage in historic stained-glass windows. Once damage thresholds have been established for a given stained-glass, the laser cleaning protocol has to be defined limiting the temperature rise during the irradiation treatment, in order to avoid deterioration of the glass as a consequence of thermal shock.

Acknowledgements

This manuscript is dedicated to the memory of Prof. Victor M. Orera, in recognition of his scientific excellence, contributions and extensive support of our Laser Laboratory community at INMA. This work was supported by European Union's

Horizon 2020 research and innovation programme under the Marie Skłodowska-Curie grant agreement N.º 766311. Partial support is obtained from Gobierno de Aragón "Construyendo Europa desde Aragón" (research group T54.20R). The use of Servicio General de Apoyo a la Investigación at the University of Zaragoza is acknowledged. This work has been performed in the framework of the Unidad Asociada de I+D+I al CSIC "Vidrio y Materiales del Patrimonio Cultural (VIMPAC)", by INMA (CSIC-University of Zaragoza) and University of Burgos.

REFERENCES

- [1] M.P. Alonso, *Vidrieras de la catedral de Burgos*, Consejo Superior de Investigaciones Científicas, 2016, ISBN: 978-84-608-8912-0.
- [2] S. Alberta, M. Gianmario, P. Valentina, The stained-glass window of the southern transept of St. Anthony's Basilica (Padova, Italy): study of glasses and grisaille paint layers, *Spectrochim. Acta Part B: At. Spectrosc.* 66 (2011) 81–87.
- [3] O. Schalm, K. Janssens, H. Wouters, D. Caluwé, Composition of 12–18th century window glass in Belgium: non-figurative windows in secular buildings and stained-glass windows in religious buildings, *Spectrochim. Acta Part B: At. Spectrosc.* 62 (2007) 663–668.
- [4] H. Rörmich, K. Dickmann, P. Mottner, J. Hildenhagen, E. Müller, Laser cleaning of stained glass windows – final results of a research project, *J. Cult. Herit.* 4 (2003) 112–117.
- [5] N. Carmona, M. Villegas, J.F. Navarro, Study of glasses with grisailles from historic stained glass windows of the cathedral of León (Spain), *Appl. Surf. Sci.* 252 (2006) 5936–5945.
- [6] M. García-Heras, N. Carmona, C. Gil, M.A. Villegas, Neorenaissance/Neobaroque stained glass windows from Madrid: a characterisation study on some panels signed by the Maumejean Frères company, *J. Cult. Herit.* 6 (2005) 91–98.
- [7] S. Brown, S. Strobl, *A Fragile Inheritance: The Care of Stained Glass and Historic Glazing: a Handbook for Custodians*, Church House Publishing, London, UK, 2002, ISBN: 9780715176009.
- [8] F. Becherini, A. Bernardi, A. Daneo, F.G. Bianchini, C. Nicola, M. Verità, Thermal stress as a possible cause of paintwork loss in medieval stained glass windows, *Stud. Conserv.* 53 (2008) 238–251.
- [9] R. Brill, Crizzling: a problem in glass conservation, in: *Conservation in Archaeology and the Applied Arts: Preprints of the Contributions to the IIC Stockholm Congress*, International Institute for Conservation of Historic and Artistic Works, 1975, pp. 121–134, ISBN: 9780950052564.
- [10] M. García-Vallés, D. Gimeno-Torrente, S. Martínez-Manent, J.L. Fernández-Turiel, Medieval stained glass in a Mediterranean climate: typology, weathering and glass decay, and associated biomineralization processes and products, *Am. Mineral.* 88 (2003) 1996–2006, <http://dx.doi.org/10.2138/am-2003-11-1244>.
- [11] C.C. Ngo, Q.H. Nguyen, T.H. Nguyen, N.T. Quach, P. Dudhagara, T.H.N. Vu, T.T.X. Le, T.T.H. Le, T.T.H. Do, V.D. Nguyen, N.T. Nguyen, Q. Phi, Identification of fungal community associated with deterioration of optical observation instruments of museums in northern Vietnam, *Appl. Sci.* 11 (12) (2021) 5351, <http://dx.doi.org/10.3390/app11125351>.
- [12] R.O. Byrne, Conservation of historic window glass, *Bull. Assoc. Preserv. Technol.* 13 (1981) 3–9, JSTOR, www.jstor.org/stable/1493959.

- [13] S. Murcia-Mascarós, P. Foglia, M.L. Santarelli, C. Roldán, R. Ibañez, A. Muñoz, P. Muñoz, A new cleaning method for historic stained glass windows, *J. Cult. Herit.* 9 (2008) e73–e80.
- [14] M. Veritá, Modern and ancient glass: nature, composition and deterioration mechanisms, in: R.A. Lefèvre (Ed.), *The Materials of Cultural Heritage in their Environment*, EDIPUGLIA, 2006, pp. 119–132.
- [15] N. Carmona, K. Wittstadt, H. Römich, Consolidation of paint on stained glass windows: comparative study and new approaches, *J. Cult. Herit.* 10 (2009) 403–409, <http://dx.doi.org/10.1016/j.culher.2008.12.004>.
- [16] R. Abd-Allah, Chemical cleaning of soiled deposits and encrustations on archaeological glass: a diagnostic and practical study, *J. Cult. Herit.* 14 (2013) 97–108, <http://dx.doi.org/10.1016/j.culher.2012.03.010>.
- [17] C. Altavilla, E. Ciliberto, S. La Delfa, S. Panarello, A. Scandurra, The cleaning of early glasses: investigation about the reactivity of different chemical treatments on the surface of ancient glasses, *Appl. Phys. A: Mater. Sci. Process.* 92 (2008) 251–255, <http://dx.doi.org/10.1007/s00339-008-4499-x>.
- [18] J.M. Delgado, D. Nunes, E. Fortunato, C.A.T. Laia, L.C. Branco, M. Vilarigues, The effect of three luminescent ionic liquids on corroded glass surfaces – a first step into stained-glass cleaning, *Corros. Sci.* 118 (2017) 109–117, <http://dx.doi.org/10.1016/j.corsci.2017.01.027>.
- [19] H. Römich, P. Mottner, J. Hildenhagen, K. Dickmann, G. Hettinger, F. Bornschein, Comparison of cleaning methods for stained glass windows, in: K. Dickmann, C. Fotakis, J.F.J.F. Asmus (Eds.), *Lasers in the Conservation of Artworks*. Springer Proceedings in Physics, vol. 100, Heidelberg, Springer, Berlin, 2005, pp. 157–161, http://dx.doi.org/10.1007/3-540-27176-7_20.
- [20] S. Siano, Principles of laser cleaning in conservation, in: M. Schreiner, M. Strlic, R. Salimbeni (Eds.), *Handbook on the Use of Lasers in Conservation and Conservation Science*, COST G7, Brussels, Belgium, 2008.
- [21] C. Fotakis, D. Anglos, V. Zafropoulos, S. Georgiou, V. Tornari, *Lasers in Preservation of Cultural Heritage: Principles and Applications*, CRC Press, 2007.
- [22] A. Zanini, V. Trafeli, L. Bartoli, The laser as a tool for the cleaning of Cultural Heritage, *IOP Conf. Ser.: Mater. Sci. Eng.* 364 (2018), <http://dx.doi.org/10.1088/1757-899X/364/1/012078>.
- [23] N. Antonopoulou-Athera, C. Kalathakis, E. Chatzitheodoridis, A.A. Serafetinides, Theoretical and experimental approach on laser cleaning of coins, *SN Appl. Sci.* 1 (2019) 238, <http://dx.doi.org/10.1007/s42452-019-0255-4>.
- [24] M. Hrnjić, *Application of Lasers for Surface Cleaning of Cultural Heritage Metals* (Master's thesis), University of Evora, Evora, 2015.
- [25] E. Basso, F. Pozzi, M.C. Relley, The Samuel F.B. Morse statue in Central Park: scientific study and laser cleaning of a 19th-century American outdoor bronze monument, *Herit. Sci.* 8 (2020) 81, <http://dx.doi.org/10.1186/s40494-020-00426-8>.
- [26] Md. Ashiqur Rahman, G.F. de la Fuente, J.M. Carretero, E.M. Maingi, M.P. Alonso Abad, R. Alonso, R. Chapoulie, N. Schiavon, L.A. Angurel, Sub-ns-pulsed laser cleaning of an archaeological bone from the Sierra de Atapuerca, Spain: a case study, *SN Appl. Sci.* 3 (2021) 865, <http://dx.doi.org/10.1007/s42452-021-04850-8>.
- [27] T. Rivas, J.S. Pozo-Antonio, A. Ramil, A.J. López, Influence of the weathering rate on the response of granite to nanosecond UV laser irradiation, *Sci. Total Environ.* 706 (2020) 135999.
- [28] P. Moretti, M. Iwanicka, K. Melessanaki, E. Dimitroulaki, O. Kokkinaki, M. Daugherty, M. Sylwestrzak, P. Pouli, P. Targowski, K.J. van den Berg, L. Cartechini, C. Miliani, Laser cleaning of paintings: in situ optimization of operative parameters through non-invasive assessment by optical coherence tomography (OCT), reflection FT-IR spectroscopy and laser induced fluorescence spectroscopy (LIF), *Herit. Sci.* 7 (2019) 44, <http://dx.doi.org/10.1186/s40494-019-0284-8>.
- [29] J. Striova, R. Fontana, I. Barbetti, L. Pezzati, A. Fedele, C. Riminesi, Multisensorial assessment of laser effects on shellac applied on wall paintings, *Sensors* 21 (2021) 3354, <http://dx.doi.org/10.3390/s21103354>.
- [30] C. Kerse, H. Kalaycioglu, P. Elahi, B. Cetin, D.K. Kesim, Ó. Akcaalan, S. Yavas, M.D. Aşik, B. Öktem, H. Hoogland, R. Holzwarth, F.Ö. Ilday, Ablation-cooled material removal with ultrafast bursts of pulses, *Nature* 537 (2016) 84–88, <http://dx.doi.org/10.1038/nature18619>.
- [31] M. Mateo, G. Nicolas, V. Pinon, A. Ramil, A. Yanez, Laser cleaning: an alternative method for removing oil-spill fuel residues, *Appl. Surf. Sci.* 247 (2005) 333–339.
- [32] F. Fekrsanati, S. Klein, J. Hildenhagen, K. Dickmann, Y. Marakis, A. Manousaki, V. Zafropoulos, Investigations regarding the behaviour of historic glass and its surface layers towards different wavelengths applied for laser cleaning, *J. Cult. Herit.* 2 (2001) 253–258, [http://dx.doi.org/10.1016/S1296-2074\(01\)01130-X](http://dx.doi.org/10.1016/S1296-2074(01)01130-X).
- [33] U. Drewello, R. Weißmann, S. Rölleke, E. Müller, S. Wuertz, F. Fekrsanati, C. Troll, R. Drewello, Biogenic surface layers on historical window glass and the effect of excimer laser cleaning, *J. Cult. Herit.* 1 (2000) 161–171, [http://dx.doi.org/10.1016/S1296-2074\(00\)00183-7](http://dx.doi.org/10.1016/S1296-2074(00)00183-7).
- [34] F. Fekrsanati, J. Hildenhagen, K. Dickmann, C. Troll, U. Drewello, C. Olainneck, UV-laser radiation: basic research of the potential for cleaning stained glass, *J. Cult. Herit.* 1 (2000) 155–160, [http://dx.doi.org/10.1016/S1296-2074\(00\)00150-3](http://dx.doi.org/10.1016/S1296-2074(00)00150-3).
- [35] H. Römich, A. Weinmann, Laser cleaning of stained glass windows. Overview on an interdisciplinary project, *J. Cult. Herit.* 1 (2000) 151–154, [http://dx.doi.org/10.1016/S1296-2074\(00\)00186-2](http://dx.doi.org/10.1016/S1296-2074(00)00186-2).
- [36] G.M. Bilmes, J. Vallejo, C. Costa-Vera, M.E. García, High efficiencies for laser cleaning of glassware irradiated from the back: application to glassware historical objects, *Appl. Phys. A: Mater. Sci. Proc.* 124 (2018) 1–11, <http://dx.doi.org/10.1007/s00339-018-1761-8>.
- [37] S.M. Eaton, H. Zhang, P.R. Herman, F. Yoshino, L. Shah, J. Bovatsek, A.Y. Arai, Heat accumulation effects in femtosecond laser-written waveguides with variable repetition rate, *Opt. Express* 13 (2005) 4708–4716.
- [38] R.R. Gattass, L.R. Cerami, E. Mazur, Micromachining of bulk glass with burst of femtosecond laser pulses at variable repetition rates, *Opt. Express* 14 (2006) 5279–5284.
- [39] H. Zhang, S.M. Eaton, J. Li, P.R. Herman, Heat accumulation during high repetition rate ultrafast laser interaction: waveguide writing in borosilicate glass, *J. Phys.: Conf. Ser.* 59 (2007) 682–686.
- [40] R. Weber, T. Graf, P. Berger, V. Onuseit, M. Wiedenmann, C. Freitag, A. Feuer, Heat accumulation during pulsed laser materials processing, *Opt. Express* 22 (2014) 11312–11324, <http://dx.doi.org/10.1364/OE.22.011312>.
- [41] J.M. Liu, Simple technique for measurements of pulsed Gaussian-beam spot sizes, *Opt. Lett.* 7 (1982) 196–198.
- [42] S. Chen, C.P. Grigoropoulos, H.K. Park, P. Kerstens, A.C. Tam, Photothermal displacement measurement of transient melting and surface deformation during pulsed laser heating, *Appl. Phys. Lett.* 73 (1998) 2093–2095.
- [43] Q. Wang, H. Chen, Y. Wang, J. Sun, Thermal shock effect on the glass thermal stress response and crack propagation, *Proc. Eng.* 62 (2013) 717–724.